Maciej Jurkowski, Leszek Łatka

The Effect of Cooling Time $t_{8/5}$ on Properties of MAG-Welded Joints Made of High-Strength Steels Using Robotic Methods

Abstract: The paper presents results of tests concerning butt welded joints made of structural high-strength steel S1100QL using a robotic welding station. The subject of the tests was to determine the effect of cooling time $t_{8/5}$ on primary mechanical properties of joints. Time $t_{8/5}$ was controlled by changing preheating temperature in relation to constant linear energy (SE specimens) and changing linear energy in relation to constant preheating temperature (ST specimens). Both of the above-named cases involved the preparation of three test plates in relation to three times, i.e. 5 seconds, 7.5 seconds and 10 seconds. The test welded joints subjected to non-destructive and destructive tests represented quality level B (in accordance with PN-EN ISO 5817). No effect of time $t_{8/5}$ on mechanical properties was noticed in terms of the ST series specimens. The tensile strength identified in the tests amounted to 1020 MPa. The specimen ruptured in the weld. However, the effect of the tensile strength on hardness was noticeable, particularly in the HAZ (even above 450 HV1). The reverse tendency could be observed in relation to the SE series specimens. The value of time $t_{8/5}$ was important in terms of joint strength, amounting to more than 1100 MPa in relation to the shortest time, where the specimen ruptured in the HAZ. In turn, the effect of time $t_{8/5}$ was negligible as regards hardness.

Keywords: high strength steels, steel S1100QL, MAG welding, robotisation, robotics, time $t_{8/5}$

DOI: *10.17729/ebis.2022.4/5*

Introduction

Presently, the fast development of automated fabrication systems often inspires investments in robotic stations aimed to increase production process efficiency, improve product quality and reduce manufacturing costs [1-3]. One of the robotisation-oriented industries is the welding sector involved in the making of large-sized elements used in the automotive industry, crane structures, and ships or in railway rolling stock [4]. Widespread robotic applications necessitate the performance of tests concerning the implementation of robotic solutions making it possible to carry out crucial tasks involving the use of high-strength materials, the yield point of which often exceeds

mgr inż. Maciej Jurkowski – Heldener Metalltechnik Polska Sp. z o.o. & Co. Sp.K,; dr hab. inż. Leszek Łatka, Professor at the Wrocław University of Science and Technology – Chair of Plastic Processing, Welding and Metrology,

1000 MPa [5]. As a result, it is possible to reduce kerb weight, material consumption and manufacturing time. However, the application of the above-named technologies and materials entails significant problems accompanying the making of high-quality joints ensuring the obtainment of required mechanical properties as well as the transfer of specific loads [6, 7]. Only a properly designed and performed welding process can provide the aforesaid materials with appropriate strength enabling the production of increasingly advanced and light structures [8].

One of the solutions to the above-presented issues could be the application of welding robots. Because of the possible improvement of production efficiency and joint quality, the robotisation of joining-related operations is increasingly popular [9]. It should be noted that a properly designed robotic line for welding applications enables return on investment within 1 to 2 years, provided that the production line operation is continuous and arc burning times are between 2 and 3 longer than those accompanying manual welding [10].

In terms of technology, the adjustment of welding parameters, including joint cooling time restricted within the range of 800°C to 500°C and referred to as $t_{8/5}$, is of great importance. The above-named cooling time affects the microstructure and mechanical properties of joints, which translates into the usability of the entire welded structure [11, 12]. Welding conditions are characterised by very fast heating and cooling rates as well as short hold times at maximum temperature. As a result, forecasting related to mechanical properties of welded joints could be problematic. For this reason, it is necessary to perform experimental and analytical tests aimed to identify structural transformations in relation to time $t_{8/5}$. Figure 1 presents a CCT diagram for welding conditions in relation to steel S1100QL.

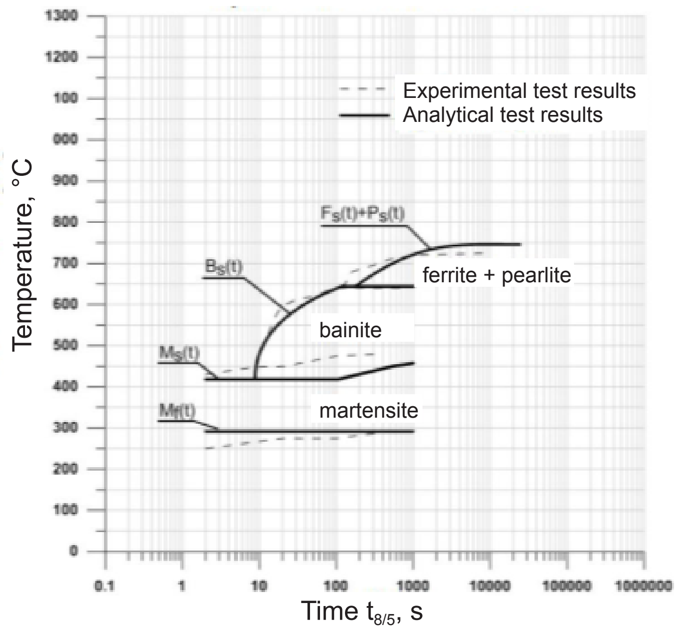

Fig. 1. CCT diagram for welding conditions in relation to steel S1100QL [13]

This article discusses possible solutions aimed to make butt joints of high-strength steel S1100QL using the M25 mixture-shielded arc welding process, a robotic welding station and variable cooling time $t_{8/5}$. The robot used in the tests was equipped with a "touch sense" type of tracking system enabling the precise and repeatable making of joints. The test joints were subsequently subjected to destructive and non-destructive tests aimed to identify the effect of cooling time $t_{8/5}$ on the structure and mechanical properties of the joints.

Materials and methods

The base material used in the tests was 12 mm thick high-strength structural steel S1100QL. The chemical composition of the steel was identified on the basis of heat analysis. The results of the heat analysis are presented in Table 1, whereas the primary mechanical properties of the steel are presented in Table 2.

The structure of the base material (typical of fine-grained martensitic steels) is presented in Figure 2.

The welded joints were made using a Union X 90 filler metal wire (EN ISO 16834-A: G 89 6 M21 Mn4Ni2CrMo) having a diameter of 1.0 mm. The chemical composition of the filler metal is presented in Table 3. The tensile strength of the filler metal amounted to 1020 MPa, whereas its elongation amounted to 16%.

Table 1. Chemical composition of steel S1100QL

Chemical element content, % by weight									
C	Si	Mn	P	S	Al	Cr	Mo	Ni	V
0.16	0.24	0.94	0.01	0.004	0.029	0.64	0.61	1.92	0.001

Table 2. Mechanical properties of steel S1100QL

Yield point R_e, MPa	**Tensile strength R_m, MPa**	**Elongation A_{min}, %**
> 1100	> 1400	11

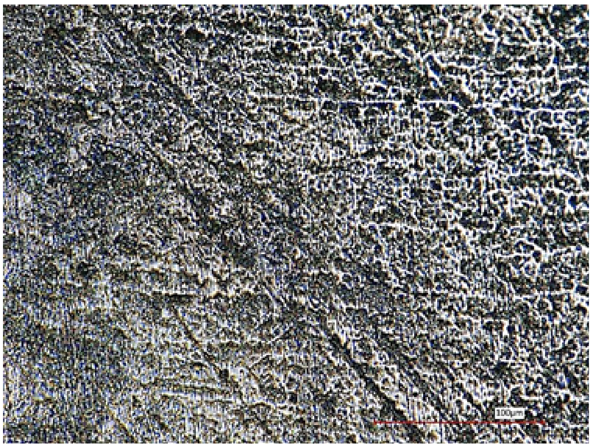

Fig. 2. Microstructure of the base material; mag. 1000x

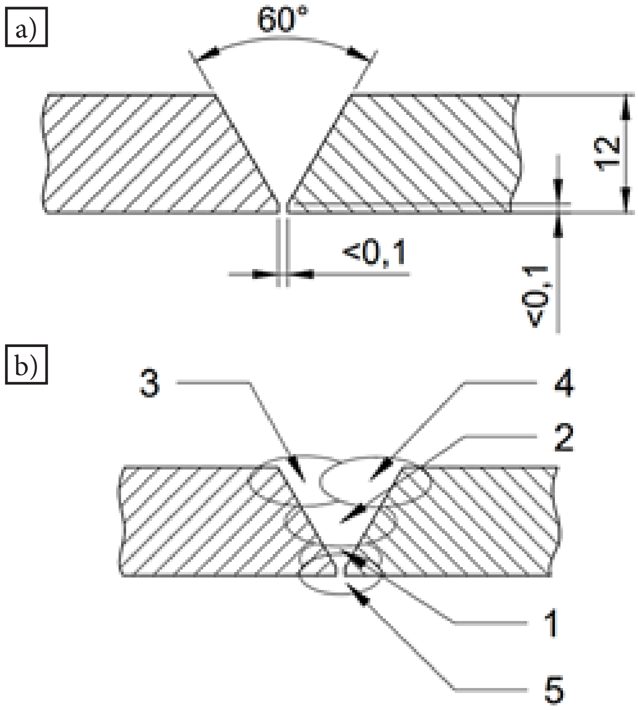

Fig. 2. Pre-weld joint preparation (a) and welding sequence (b)

The joints of the test plates (600 mm x 300 mm x 12 mm) were welded using the MAG method, a robotic welding station provided with an ARC Mate 0iB 6-axis robot (Fanuc) and a TPS 500i welding power source (Fronius). The ISO 14175-M25-ArCO-13/4 shielding gas used in the tests aimed to increase the flowing power of the weld pool and the efficiency of the welding process. The plate edge bevelling method and the welding sequence are presented in Figure 2.

The tests involved the making of six test joints in two series: (i) SE series (involving the application of constant linear energy and variable preheating temperature) and (ii) ST series (connected with the use of constant preheating temperature and variable linear energy). In both cases, the times of cooling from 800°C to 500°C ($t_{8/5}$) amounted to 5 s, 7.5 s and 10 s. Time $t_{8/5}$ was determined analytically using the formula for the two-dimensional flow of heat in accordance with the PN-EN 1011-2 standard. The designations of the specimens along with primary parameters are presented in Table 4. The interpass temperature was equal to preheating temperature in relation to a given experiment.

After 24 hours, the test joints were subjected to non-destructive tests, i.e. visual tests (performed in accordance with PN-EN ISO 17637), magnetic particle tests (performed in accordance with PN-EN ISO 17638) and ultrasonic tests (performed in accordance with PN-EN ISO 17640). Afterwards, the test plates were

Table 3. Chemical composition of the Union X 90 filler metal wire

Chemical element content, % by weight									
C	Si	Mn	P	S	Ni	Mo	Cr	Cu	V
0.10	0.79	1.76	0.011	0.008	2.10	0.58	0.39	0.13	0.01

Table 4. Specimen designation

Specimen designation	Linear energy, kJ/mm	Preheating temperature, °C	Time $t_{8/5}$, s
T5SE	0.82	55	5
T7.5SE	0.82	120	7.5
T10SE	0.82	170	10
T5ST	0.71	120	5
T7.5ST	0.82	120	7.5
T10ST	0.94	120	10

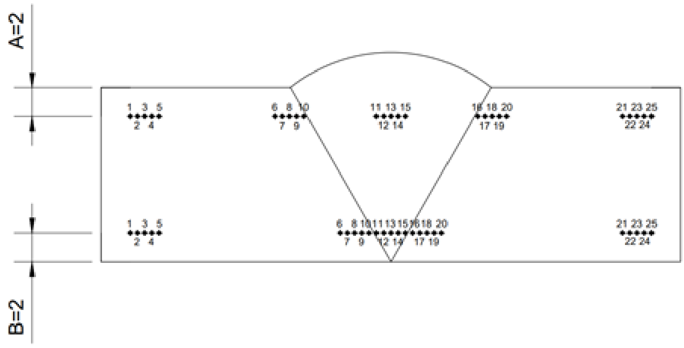

Fig. 3. Arrangement of hardness measurement points in the welded joints

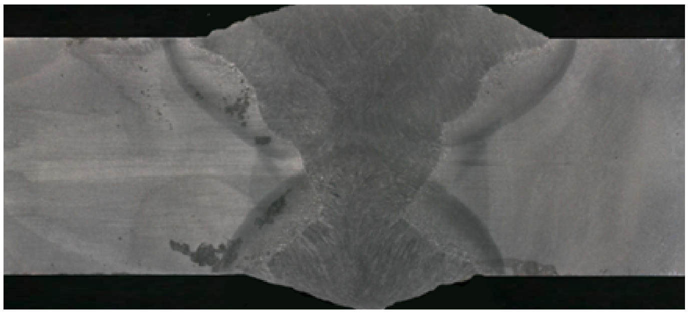

Fig. 4. Macrostructure of specimen T5SE; mag. 20x, etchant: Adler

subjected to destructive tests. Metallographic tests were performed in accordance with the PN-EN ISO 17639 standard. The specimens were subjected to grinding, polishing and etching in Adler's reagent. Microscopic observations were performed using a VHX6000 microscope (Keyence). Tensile tests were performed in accordance with the PN-EN ISO 4136 standard using a T008/SK testing machine. Hardness measurements were performed in accordance with the PN-EN ISO 9015-2 standard using the Vickers hardness tests, an indenter load force of 9.81 N (HV1) and a Sinowon hardness tester. The schematic diagram of measurement points is presented in Figure 3.

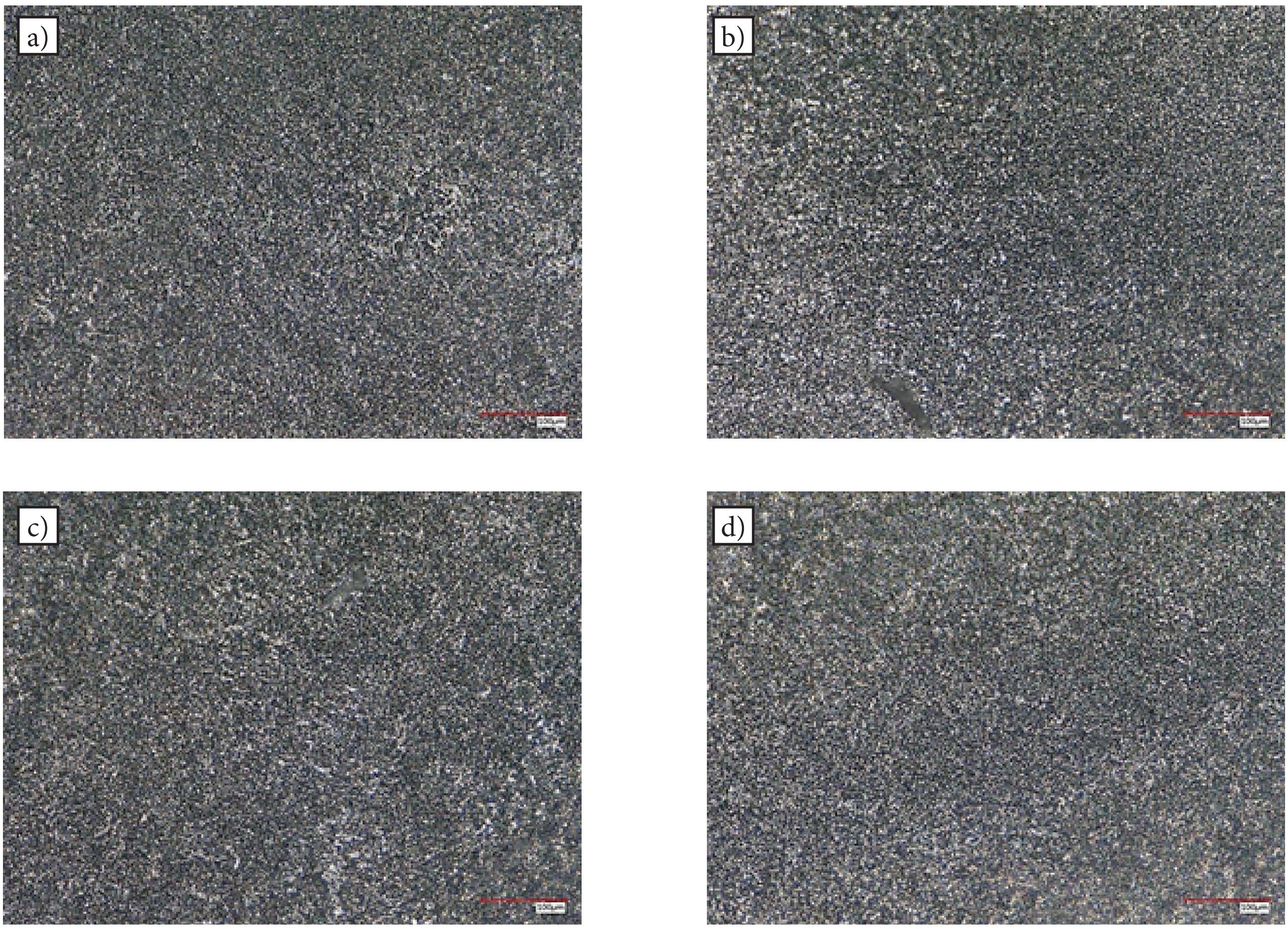

Fig. 5. Microstructure of the test joints: a), c) – filling run in T5SE and T10SE, b), d) – HAZ in T5SE and T10SE

Results

The macroscopic observations of the welded joints (Figure 4) revealed that the arrangement of the beads was consistent with the welding technology. In addition, the macroscopic tests revealed that the material did not contain any discontinuities (cracks). It was possible to notice two weld faces and the smooth interface between them and the base material, which implied that the joints were characterised by satisfactory fatigue strength [12].

The microscopic observations of the SE series specimens (Fig. 5) confirmed the presence of tempered martensite as the result of the multi-run welding process, where each bead tempered the previous one, preventing also the partial martensitic transformation.

In turn, it was possible do observe differences in relation to the ST series specimens (Fig. 6). Specimen T5ST contained the martensitic structure, which could be the reason for higher hardness and strength. In turn, specimen T10ST contained areas of bainite (decreasing hardness but increasing plasticity). The structures obtained in the tests were similar to those discussed in related reference publications [13].

The tensile test results are presented in Figure 7. As can be seen, all of the specimens were characterised by tensile strength lower than that of the base material (1400 MPa). In most cases, the rupture took place in the weld. Specimen T5SE was characterised by slightly higher tensile strength than the ultimate immediate strength of the filler metal. In addition, in the above-named case, the specimen ruptured in the HAZ.

In addition, the analysis of the test results revealed the clearly noticeable effect of time $t_{8/5}$ on the strength of the joints in the SE series specimens. The foregoing resulted from the fact that the change of preheating temperature and that of the interpass temperature affected the rate of heat flow inside the material. An increase in the cooling time was accompanied by a decrease

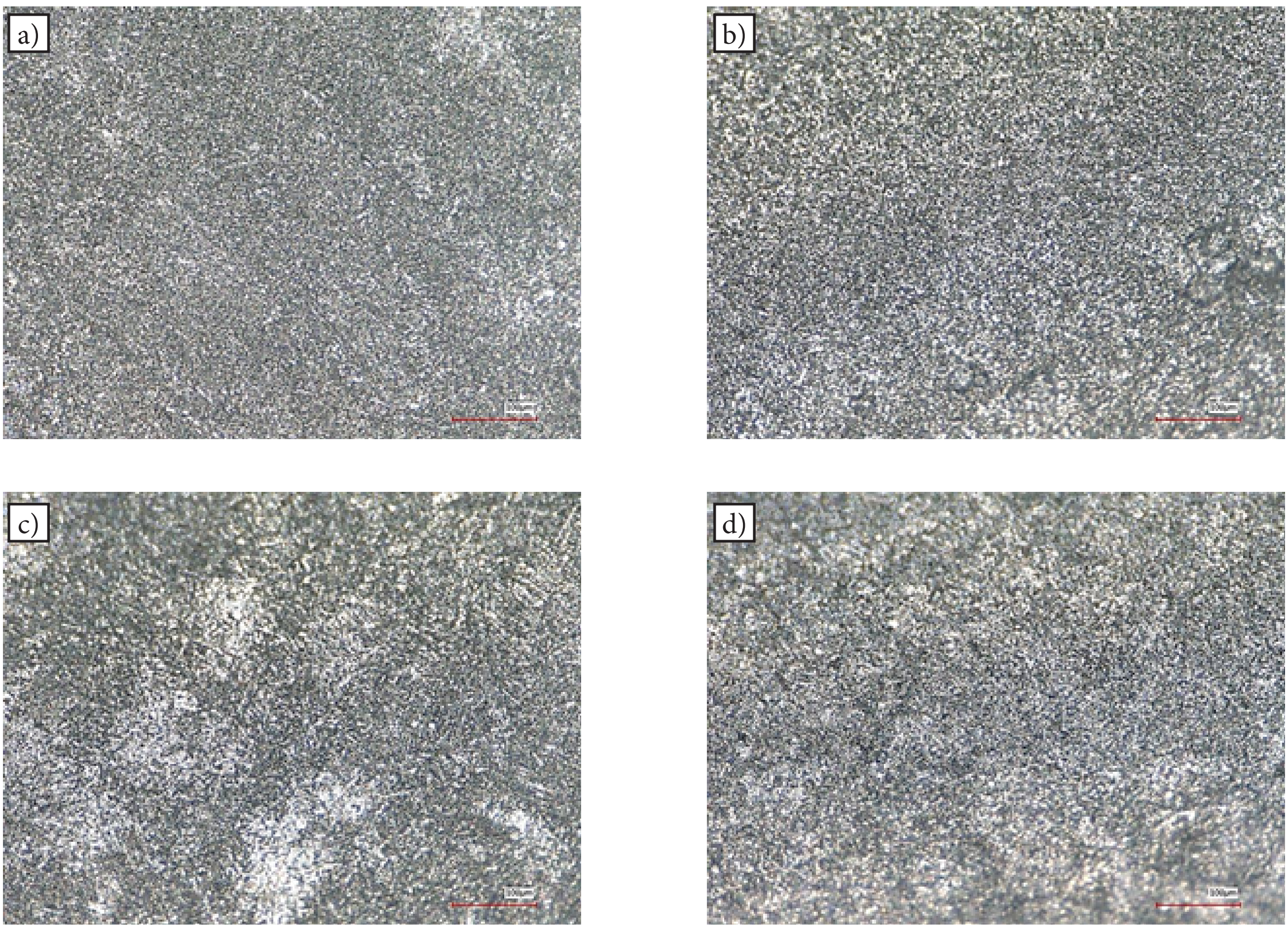

Fig. 6. Microstructure of the test joints: a), c) – filling run in T5ST and T10ST, b), d) – HAZ in T5ST and T10ST

in tensile strength. The reduction of tensile strength was connected with the growth of grains and easier grain boundary sliding. In turn, as regards the ST series specimen, the change of cooling time $t_{8/5}$ did not ma significantly affect the tensile strength of the joints. The foregoing could be attributed to relatively high (120°C) preheating temperature and interpass temperature, significantly slowing down the flow of heat inside the material and precluding the formation of the significantly more fine-grained structure [14, 15].

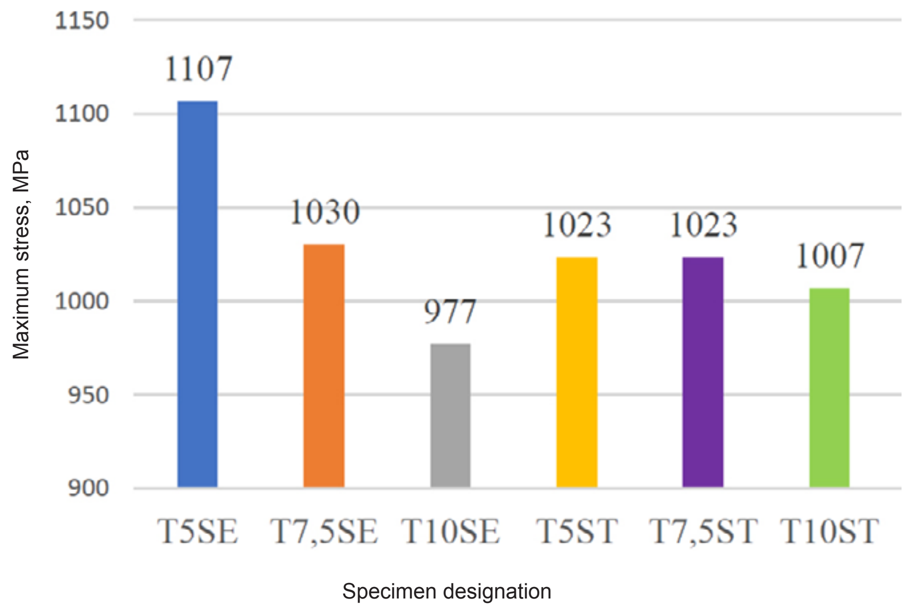

Fig. 7. Maximum stress values obtained in the tensile tests

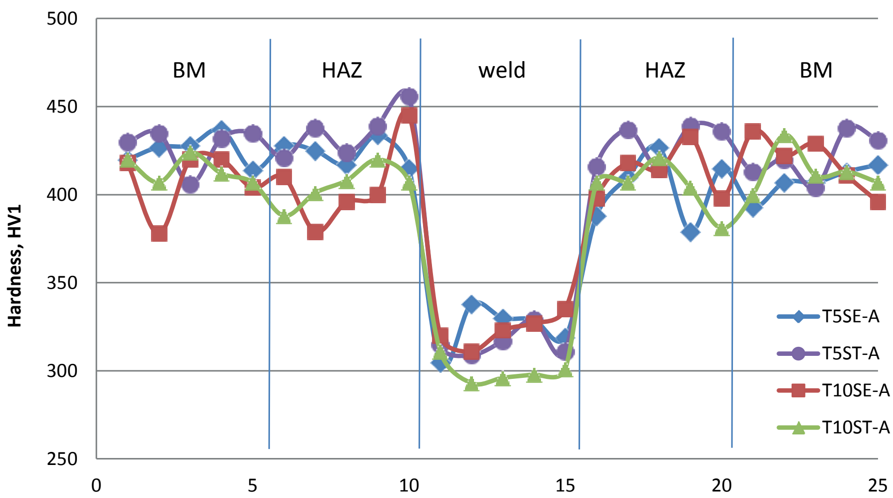

Fig. 8. Hardness test results (line A in accordance with Fig. 3)

The hardness measurements revealed that, in terms of the SE series specimen, the change of time $t_{8/5}$ did not significantly affect the hardness of the HAZ and that of the weld. The above-named phenomenon resulted from the use of the welding method (multi-run welding), where each bead tempered the previous one, preventing the partial martensitic transformation. A greater effect on hardness could be observed in the ST series specimens. Specimen T5ST was characterised by the highest average HAZ hardness in relation to all tests results (above 450 HV1). The foregoing resulted from a small heat input and, consequently, the shortest cooling time of each bead. The low heat input and short cooling time precluded the tempering of previous beads, which resulted in partial martensitic transformation [16, 17]. The values obtained in the tests (Fig. 8) satisfied the requirements specified in the PN-EN ISO 15614-1 standard, stating that the maximum hardness of steels from group 3 should amount to 450 HV10. However, it should be noted that specific values apply to steels where $R_e > 890$ MPa.

The analyses of chemical composition were performed using a spark emission spectrometer (Spectrotest, Spectro Poland). The chemical elements which underwent the most intense burnout were silicon and manganese (approximately 1/3 of the initial content). In turn, the longer the time $t_{8/5}$, the (slightly) lower the burnout degree. The tests also revealed that chromium and copper were burnt out to a lesser extent, whereas there was no clearly visible burnout of nickel, molybdenum and vanadium.

Concluding remarks

The above-presented test results justified the formulation of the following conclusions:

– gas-shielded arc butt welding technology developed to join 12 mm thick plates made of

steel S1100QL ensured the obtainment of high quality joints (verified in subsequently performed tests),
- use of the robotic welding station provided necessary process stability and ensured the obtainment of highly aesthetic and smooth welded joints,
- use of the M25 mixture made it possible to increase the flowing power of the weld pool and did not significantly contribute to the burnout of alloying elements, thus ensuring the obtainment of the proper joint structure,
- tests discussed in the article did not reveal the significant effect of cooling time $t_{8/5}$ on the hardness of the structures obtained in the tests with a constant heat input and variable preheating temperature. In turn, it was possible to observe the significant effect of cooling time $t_{8/5}$ on the hardness of the structures obtained in the tests with constant preheating temperature and a variable heat input,
- in terms of the SE series specimens, the Vickers hardness tests revealed that the change of cooling time $t_{8/5}$ significantly affected the strength of the joints, where the extension of the cooling time was accompanied by a decrease in strength,
- in terms of the SE series specimens, the change of cooling time $t_{8/5}$ did not significantly affect the strength of the joints,
- more favourable method applied to control cooling time $t_{8/5}$ was the one where a heat input was constant and preheating temperature was variable. The use of the above-named method prevented the formation of hard structures characterised by partial martensitic transformation and enabled the obtainment of favourable mechanical properties of the test joints.

References

[1] Tasak E.: Metalurgia Spawania, Wydawnictwo JAK, Kraków 2008.

[2] Butnicki S.: Spawalność i kruchość stali, WNT, Warszawa 1991.

[3] Pickering F.B.: Physical metallurgy and the design of steels, University of Michigan, 1978.

[4] Tasak E., Ziewiec A.: Spawalność materiałów konstrukcyjnych. Tom 1. Spawalność stali, Wydawnictwo JAK, Kraków 2009.

[5] Tuz L., Sulikowski K.: Ocena możliwości spawania wiązką laserową stali ulepszanej cieplnie o granicy plastyczności 1100 MPa, Biuletyn Instytutu Spawalnictwa, 2019, no. 6, pp. 25-31.

[6] Brózda J., Jachim R., Kwieciński K., Łomozik M., Węglowski M.St.: Stale konstrukcyjne i ich spawalność, Instytut Spawalnictwa, Gliwice 2017.

[7] Łomozik M., Turyk E.: Właściwości mechaniczne złączy spawanych stali S1100QL po wielokrotnym spawaniu naprawczym, Biuletyn Instytutu Spawalnictwa, 2018, no. 3, pp. 21-25.

[8] Mochozuki M., Shintomi T., Haskimoto Y., Toyada M.: Analytical study on deformation and strength in HAZ-softened welded joints of fine grained steels, Welding in the World, 2004, vol. 48, pp. 2-12.

[9] Norberto Pires J., Loureiro A., Bölmsjo G.: Welding robots: technology, system issues and applications, University of Coimbra, 2006.

[10] Siennicki A.: Perspektywy rozwoju robotyzacji spawania łukowego w osłonie gazowej, Przegląd Spawalnictwa, 2011, no. 8, pp. 3-8.

[11] Sajek A.: Welding thermal cycles of joints made of S1100QL steel by SAW and hybrid plasma-MAG processes, Advances in Materials Science, 2020, vol. 20(4), pp. 75-86.

[12] Kowalski M., Łagoda T., Żok F., Chmelko V.: Fatigue life of butt weldments made of S1100QL steel, Journal of Machine Construction and Maintance, 2019, vol. 2, pp. 7-13.

[13] Piekarska W., Saga M., Goszczańska-Króliszewska D., Domański T., Kopas P.: Application of analytical methods for determination of hardness distribution in welded joint made of S1100QL steel, MATEC Web of Conferences 157, 2018.

[14] Nowacki J., Sajek A., Matkowski P.: The influence of welding heat input on the microstructure of joints of S1100QL steel in one-pass welding, Archives of Civil and Mechanical Engineering, 2016, vol. 16, pp. 777-783.
[15] Samardzic I., Coric A., Dunder M.: Weldability investigation of fine-grained S1100QL steel, Metalurgija, 2016, vol. 55(3), pp. 453-456.
[16] Łomozik M.: Mikrostruktura, udarność i twardość SWC stali S1100QL po symulacji oraz w rzeczywistym złączu spawanym metodą MAG drutem elektrodowym proszkowym o rdzeniu metalicznym, Biuletyn Instytutu Spawalnictwa, 2021, no. 5, pp. 47-65.
[17] Brabec J., Jezek S., Benes L., Kriz A., Majrich P.: Suitability confirmation for welding ultra-high strength steel S1100QL using the RapidWeld method, Manufacturing Technology, 2021, vol. 21(1), pp. 29-36.